

- (11) M. C. Weiss, B. Bursten, S.-M. Peng, and V. L. Goedken, *J. Am. Chem. Soc.*, **98**, 8021 (1976).
- (12) J. Keruohan and J. F. Endicott, *Inorg. Chem.*, **9**, 1504 (1970).
- (13) J. F. Endicott, J. Lilie, J. M. Kuszej, B. S. Ramaswamy, W. G. Schmonsees, M. G. Simic, M. Glick, and D. P. Rillema, *J. Am. Chem. Soc.*, **99**, 429 (1977).
- (14) J. F. Endicott, G. Ferraudi, and J. Barber, Jr., *J. Phys. Chem.*, **79**, 630 (1975).
- (15) J. F. Endicott in "Concepts in Inorganic Photochemistry", A. W. Adamson and P. D. Fleishauer, Ed., Wiley, New York, N.Y., 1975.
- (16) C. G. Hatchard and C. A. Parker, *Proc. R. Soc. London, Ser. A*, **235**, 518 (1956).
- (17) G. Ferraudi, J. F. Endicott, and J. Barber, *J. Am. Chem. Soc.*, **97**, 6406 (1975).
- (18) G. Ferraudi and J. F. Endicott, *Inorg. Chem.*, **12**, 2389 (1973), and references therein.
- (19) W. Wolfrom, *Methods Carbohydr. Chem.*, **1** (1962).
- (20) W. V. Sherman, *J. Phys. Chem.*, **71**, 1695 (1967).
- (21) H. B. Jonassen, J. B. Crumpler, and T. D. O'Brien, *J. Am. Chem. Soc.*, **67**, 1709 (1945).
- (22) J. Fries, "Analysis of Traces", E. Merk, Darmstadt, 1971.
- (23) J. G. Martin, R. M. Wei, and S. Cummings, *Inorg. Chem.*, **11**, 475 (1972).
- (24) D. A. House and N. F. Curtis, *J. Am. Chem. Soc.*, **84**, 3248 (1962).
- (25) D. K. Cabbines and D. W. Margerum, *J. Am. Chem. Soc.*, **92**, 2155 (1970).
- (26) N. F. Curtis, *J. Chem. Soc., Dalton Trans.*, 1358 (1972).
- (27) Appropriate synthetic routes were not found for the photolysis products. Chemical reduction (BH_4^- ; H_2/Ni) of either $\text{Cu}[13\text{-At}]^+$ or $\text{Cu}[13\text{-AtH}]^{2+}$ produces metallic copper. Besides, chemical oxidants^{28,29} either produce no reaction (Ph_3CBF_4) or give a complex mixture of products (Br_2).
- (28) C. Hipp, L. F. Lindoy, and D. H. Busch, *Inorg. Chem.*, **11**, 1988 (1972).
- (29) T. D. Truex and R. H. Holm, *J. Am. Chem. Soc.*, **94**, 4529 (1972).
- (30) S. Sundarajan and E. L. Wehry, *J. Phys. Chem.*, **76**, 1528 (1972).
- (31) D. C. Olson and J. Vasilekiskis, *Inorg. Chem.*, **10**, 463 (1971).
- (32) Steady-state treatment was applied to Cu(III) and radical species according to A. A. Frost and R. G. Pearson, "Kinetics and Mechanisms", Wiley, New York, N.Y., 1961.
- (33) J. F. Endicott, J. M. Plamer, and E. Papaconstantinou, *Inorg. Chem.*, **8**, 1516 (1969).
- (34) For a review of the photochemical properties and absorption spectra of organic compounds with imino groups see A. Padwa, *Chem. Rev.*, **77**, 37 (1977).

Contribution from the Department of Chemistry,
University of California, Santa Barbara, California 93106

Photochemistry of the Ruthenium(II)-Saturated Amine Complexes $\text{Ru}(\text{NH}_3)_6^{2+}$, $\text{Ru}(\text{NH}_3)_5\text{H}_2\text{O}^{2+}$, and $\text{Ru}(\text{en})_3^{2+}$ in Aqueous Solution

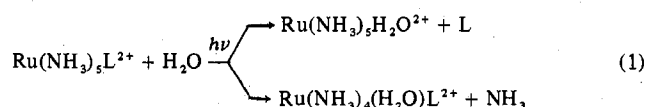
TADASHI MATSUBARA¹ and PETER C. FORD*²

Received December 16, 1977

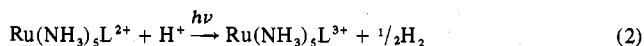
Photolysis of $\text{Ru}(\text{NH}_3)_6^{2+}$ in aqueous solution leads to products which can be attributed to two independent, primary photoreactions: aquation of coordinated ammonia and oxidation of Ru(II) to Ru(III) with concomitant formation of H_2 . At longer irradiation wavelengths (313–405 nm), which correspond to ligand field absorption bands, photoaquation predominates and gives wavelength-independent quantum yields ($\Phi_{\text{aq}} = 0.26 \pm 0.1$ mol/einstein). Wavelength-independent photooxidation ($\Phi_{\text{ox}} \sim 0.03$) is also seen in this region, and it is argued that the latter pathway is the result of the back-population from a common LF state into a higher energy charge transfer to solvent state. For $\lambda_{\text{irr}} < 313$ nm, a sharp increase in Φ_{ox} and simultaneous decrease in Φ_{aq} is noted. At these wavelengths excitation corresponds to direct absorption into a band attributed to a CTTS transition. For 254-nm photolysis Φ_{ox} is found to be 0.36 and the ratio $\Phi_{\text{ox}}/\Phi_{\text{H}_2}$ is ~ 2 . Quantum yield effects of $[\text{H}^+]$ and 2-propanol are interpreted in terms of the reaction of the CTTS excited state with H^+ to give Ru(III) plus a hydrogen atom, a species which may lead to the oxidation of a second Ru(II) complex or may be trapped by 2-propanol when the latter is present. Qualitatively, the photolysis behaviors of aqueous $\text{Ru}(\text{NH}_3)_5\text{H}_2\text{O}^{2+}$ and $\text{Ru}(\text{en})_3^{2+}$ are similar but several significant differences are evident. No photoaquation of NH_3 is seen for $\text{Ru}(\text{NH}_3)_5\text{H}_2\text{O}^{2+}$, and photolabilization, if present, must be confined to the spectrally undetectable exchange of solvent and coordinated H_2O . For $\text{Ru}(\text{en})_3^{2+}$ the photoaquation pathway for the longer λ_{irr} is wavelength dependent indicating that a higher energy state is particularly photoactive toward ligand labilization. The photochemical technique is employed to synthesize the monodentate ethylenediaminium complex ions $\text{Ru}(\text{en})_2(\text{enH})\text{Cl}^{3+}$ and $\text{Ru}(\text{en})_2(\text{Hen})(\text{H}_2\text{O})^{3+}$, and their properties are described.

Introduction

Earlier studies have demonstrated a wide variety of photochemical reactivities for ruthenium(II) complexes^{3–8} with the pentaammine complexes $\text{Ru}(\text{NH}_3)_5\text{L}^{2+}$ receiving particular attention in this laboratory.^{3–6} When L is a π -unsaturated ligand such as pyridine, acetonitrile, or dinitrogen, the spectra display intense metal-to-ligand charge-transfer (MLCT) absorptions.⁹ In some cases, irradiation produces photochemistry consistent with the formulation of the MLCT states as an oxidized metal center coordinated to a radical ion ligand $[(\text{NH}_3)_5\text{Ru}^{\text{III}}(\text{L}^-)]^{2+}$, examples being the photoexchange¹⁰ between the solvent and the pyridine hydrogens of $\text{Ru}(\text{NH}_3)_5\text{py}^{2+}$ and the electron-transfer photochromism seen for the pyrazine complex $\text{Ru}(\text{NH}_3)_5\text{pz}^{2+}$ in the presence of cupric ion.^{4b} However, more common reaction modes in aqueous solutions are ligand photoaquation (eq 1) or oxidation of



Ru(II) to Ru(III) with simultaneous H_2 formation (eq 2).



These pathways have been attributed to the population of ligand field (LF) excited states^{4–6,10} and of charge transfer to solvent (CTTS) excited states,⁶ respectively. Such arguments suffer major ambiguity given the fact that the intense MLCT and internal ligand (IL) bands of the π -unsaturated L's generally obscure the spectral regions where the LF and CTTS absorptions are expected. Consequently, it was deemed necessary to examine the spectral and photochemical properties of Ru(II) complexes having only saturated ligands. Here are reported the photochemistries of $\text{Ru}(\text{NH}_3)_6^{2+}$, $\text{Ru}(\text{en})_3^{2+}$, and $\text{Ru}(\text{NH}_3)_5\text{H}_2\text{O}^{2+}$ in aqueous solution; elsewhere,¹¹ are described spectral properties of $\text{Ru}(\text{NH}_3)_6^{2+}$ and $\text{Ru}(\text{en})_3^{2+}$.

Experimental Section

Materials. Hexaammineruthenium(II) chloride, $[\text{Ru}(\text{NH}_3)_6]\text{Cl}_2$, was synthesized by the procedure of Lever and Powell.¹² Purification was carried out as follows. A 0.5-g portion of $[\text{Ru}(\text{NH}_3)_6]\text{Cl}_2$ (1.8×10^{-3} mol), 0.7 g of ammonium chloride, and 0.1 g of zinc powder

Table I. Absorption Spectra of Ruthenium Complexes in Aqueous Solution^a

Complex ion	λ_{max} , nm	ϵ , M ⁻¹ cm ⁻¹
Ru(NH ₃) ₆ ²⁺	390 sh	35
	275	640
Ru(NH ₃) ₅ H ₂ O ²⁺	415	40
	268	581
Ru(en) ₃ ²⁺	370 sh	120
	302	1020
<i>cis</i> -Ru(NH ₃) ₄ (H ₂ O) ₂ ²⁺	435	54
	261	530
<i>trans</i> -Ru(NH ₃) ₄ (H ₂ O) ₂ ²⁺	272	499
	385	118
Ru(enH)(en) ₂ (H ₂ O) ³⁺	290	740
	343	1880

^a Values measured at 25 °C in 0.001 M HCl/0.199 M NaCl aqueous solution.

(1.5×10^{-3} mol) were mixed in a three-neck flask. After deaerating the flask with argon, 8 mL of deaerated hot (70 °C) 1:1 aqueous NH₃ was added to dissolve the crystals. The hot solution was filtered under argon and then cooled in an ice bath. Bright yellow crystals appeared immediately. After 30 min, the crystals were filtered under argon and immediately washed with the mother liquor, deaerated cold 1:1 aqueous ethanol, ethanol, and ether. The yield of the twice recrystallized material was 0.4 g (38% overall) after drying under vacuum overnight. Anal. Calcd for H₁₈N₆Cl₂Ru: Cl, 25.8; Ru, 36.9. Found: Cl, 25.6; Ru, 36.8.

The electronic spectrum of recrystallized [Ru(NH₃)₆]Cl₂ (Table I) agrees well with a previous report,¹³ as does the IR spectrum.¹⁴ The complex was kept in a freezer over desiccant to slow possible decomposition. The electronic spectrum of the complex kept in this manner for 2 years was identical with that of a fresh sample.

Aquopentaammineruthenium(II) hexafluorophosphate monohydrate, [Ru(NH₃)₅H₂O](PF₆)₂·H₂O, was synthesized using the method of Callahan, Brown, and Meyer.¹⁵ The electronic spectrum (Table I) matches that reported,⁶ and the ruthenium analysis is consistent with the above formula. Anal. Calcd for H₁₁N₅O₂P₂F₁₂Ru: Ru, 19.7. Found: Ru, 19.5. Even when stored under vacuum in a freezer, the complex underwent slow decomposition; thus, it was prepared freshly within 1 week of use in any experiments.

Tris(ethylenediamine)ruthenium(II) tetrachlorozincate, [Ru(en)₃]ZnCl₄, was synthesized according to the published procedures¹³ and recrystallized as follows. A 0.5-g portion of the crude crystals (1×10^{-3} mol) was dissolved in 8 mL of deaerated aqueous hydrochloric acid and 0.05 g of zinc powder (8×10^{-4} mol) was added. The solution was filtered under argon atmosphere while hot. After cooling in an ice bath, 1 mL of deaerated concentrated HCl was added slowly. Light yellow crystals appeared upon cooling in an ice bath. These were collected by filtration under argon and then washed with deaerated cold ethanol and ether. This procedure was repeated twice, and the resulting light yellow material was dried under vacuum overnight. The electronic spectrum (Table I) agrees well with that reported¹³ and a satisfactory analysis was obtained. Anal. Calcd for C₆H₂₄N₆Cl₄ZnRu: C, 14.8; H, 4.9; N, 17.2; Cl, 29.0; Ru, 20.7. Found: C, 14.6; H, 4.9; N, 17.1; Cl, 30.8; Ru, 20.4. The complex salt was stable when stored over desiccant in a freezer for a period of 2 years.

Chlorobis(ethylenediamine)ethylenediamineruthenium(II) chloride tetrachlorozincate, [Ru(enH)(en)₂]Cl₂·ZnCl₄, was synthesized photolytically. A 0.2-g sample of [Ru(en)₃]ZnCl₄ (4×10^{-4} mol) was placed into a quartz tube closed with a syringe cap, and the tube was deaerated by flushing with argon. Deaerated 0.02 M HCl (35 mL) was added via syringe, and the resulting solution was photolyzed with four low-pressure mercury lamps (Ultra-Violet Products, Model PCQ X1) at 5 °C for 40 h with stirring. The greenish yellow solution was then concentrated to dryness in a rotary evaporator. The solid obtained was redissolved in hot (70 °C) aqueous 0.1 M HCl/0.1 M ZnCl₂ solution (4 mL), ethanol (2 mL) was added, and the solution was left in a freezer overnight whereupon a yellow powder separated from the green solution. This was collected by filtration and then washed with ethanol and ether. The yield after drying under vacuum was 0.10 g. The crude material was dissolved in 3 mL of hot (70 °C) 0.001 M aqueous HCl, and then concentrated HCl (2 mL) was added to precipitate the product. The solid was collected

by filtration and rinsed with ethanol and ether. This procedure was repeated twice and the yield after drying under vacuum was 0.07 g (31% overall). Anal. Calcd for C₆H₂₅N₆Cl₆ZnRu: C, 12.9; H, 4.5; N, 15.0; Cl, 37.9; Ru, 18.0. Found: C, 12.9; H, 4.6; N, 15.0; Cl, 37.7; Ru, 17.3. This material was stored over desiccant in a refrigerator since it decomposed slowly at room temperature.

The chloride salt [Ru(enH)(en)₂]Cl₃, was obtained by cation-exchange chromatography. A 0.2-g sample of [Ru(enH)(en)₂]Cl₂·ZnCl₄ was dissolved in 5 mL of 0.001 M aqueous HCl and was loaded on a column of H⁺ form Bio-Rad AG50W-X2 (200–400 mesh) resin. The column was first eluted with 2 M HCl until all zinc (detected with an aqueous K₄[Fe(CN)₆]) to form white insoluble Zn₂[Fe(CN)₆]) was washed off. The column was then eluted with 2.5 M HCl. The fractions were checked spectrophotometrically and concentrated to dryness in a rotary evaporator. The resulting hygroscopic solids were stored over desiccant in a refrigerator.

The aquobis(ethylenediamine)ethylenediamineruthenium(II) ion, Ru(enH)(en)₂H₂O³⁺, was obtained in situ by the reduction of Ru(enH)(en)₂Cl₃⁺. A sample of several milligrams of [Ru(enH)(en)₂]Cl₂·ZnCl₄ was dissolved in 10 mL of 0.01 M aqueous HCl, and the solution was deaerated with argon in a Zwickel flask. After 20 min, several pieces of Zn(Hg) were introduced, and the complex was allowed to react for 30 min before transferal under argon to a quartz spectrometer cell to obtain the electronic spectrum (Table I).

The *cis*- and *trans*-diaquotetraammineruthenium(II) ions, *cis*- and *trans*-Ru(NH₃)₄(H₂O)₂²⁺, were obtained in a similar manner by the reduction of *cis*- and *trans*-Ru(NH₃)₄Cl₂⁺, respectively. The electronic spectra of *cis*- and *trans*-Ru(NH₃)₄(H₂O)₂²⁺ obtained are summarized in Table I. The PF₆⁻ salts could be synthesized using the same procedure as for [Ru(NH₃)₅H₂O](PF₆)₂·H₂O; however, the diaquo complexes decomposed much more readily than the monoquo complex even when stored under vacuum at freezer temperature.

Photolysis Techniques. Photolyses were carried out at 405, 366, 334, 313, and 280 nm using a 200-W high-pressure mercury lamp as a source and Oriel interference filters for wavelength selection. Irradiation at 254, 228.8, and 213.9 nm was obtained from low-pressure mercury, cadmium, and zinc lamps, respectively, with wavelength selection as described by Hintze.^{6,17} Ferrioxalate actinometry was used with all wavelengths except 228.8 and 213.9 nm where uranyl oxalate actinometry was employed.⁶

The Ru(II) complexes studied here are air sensitive, so all photolysis solutions were prepared in the dark under argon deaerated conditions. Except where noted, all photolyses were carried out at 25 °C for complexes irradiated in stirred aqueous solutions with an ionic strength of 0.2 M (HCl/NaCl).

Quantum yields were determined from spectral changes measured in quartz cells using a Cary 14 or a Cary 118 spectrophotometer and were corrected for spectral changes (generally small) in an identically prepared dark reaction solution. Inner filter effects were compensated and secondary photolysis was minimized by limiting the extent of reaction and by extrapolating stepwise quantum yields to 0% reaction.¹⁸

Hydrogen was identified as a reaction product of 254-nm photolysis by analysis of evolved gases with an AE1 MS-902 mass spectrometer. Quantum yields of gas evolution were measured using a gas microvolumeter similar to that designed by Davis and Stevenson.¹⁹ Stirred, hydrogen deaerated aqueous solutions (0.01 M HCl/0.19 M NaCl) of the appropriate Ru(II) complex in thermostated, water-jacketed quartz cells (25.0 °C) were irradiated with four low-pressure mercury lamps (Ultra-Violet Products Model PCQ X1). Changes in the gas volume were measured periodically and the ideal gas law was used to calculate the number of moles of H₂ evolved. This value was compared to the number of moles of ruthenium(III) produced simultaneously in the photolysis solution as determined by spectral changes.

Results

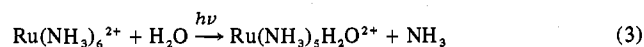
A. Photolysis of Ru(NH₃)₆²⁺. Irradiation of aqueous Ru(NH₃)₆²⁺ at wavelengths ranging from 405 to 214 nm results in photooxidation of Ru(II) to Ru(III) and in photosubstitution of coordinated ammonia. The quantum yields are irradiation wavelength (λ_{irr}) dependent with photosubstitution being the dominant pathway at $\lambda_{\text{irr}} \geq 313$ nm while photooxidation dominates at $\lambda_{\text{irr}} \leq 280$ nm. Quantum yields for these processes can be obtained from spectral data according to the following analysis.^{6,7}

Table II. Quantum Yields^a Measured for the Photolysis of Aqueous Ru(NH₃)₆²⁺

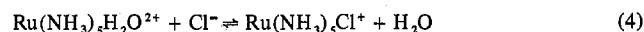
λ_{irr} , nm	Φ_{ox} , mol/einstein	Φ_{aq} , mol/einstein
405	0.025 ± 0.003 (0.019 ± 0.007) ^b	0.27 ± 0.05 (0.21 ± 0.05) ^b
366	0.022 ± 0.003 (0.016 ± 0.002) ^b (0.036 ± 0.003) ^c	0.26 ± 0.03 (0.23 ± 0.03) ^b (0.28 ± 0.02) ^c
334	0.028 ± 0.003	0.25 ± 0.02
313	0.036 ± 0.003	0.25 ± 0.03
280	0.25 ± 0.02	0.04 ± 0.01
254	0.36 ± 0.07 (0.13 ± 0.01) ^d	0.06 ± 0.01 (0.03 ± 0.01) ^d
229	0.52 ± 0.01	0.08 ± 0.01
214	0.49 ± 0.02	0.08 ± 0.02

^a Measured in 0.001 M HCl/0.199 M NaCl, 25.0 °C, unless otherwise stated; mean value and average for three or more runs under identical conditions reported. ^b At 6.0 °C. ^c Measured in 0.010 M HCl/0.190 M NaCl. ^d In 2 M 2-propanol.

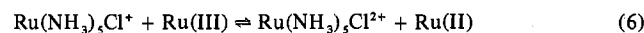
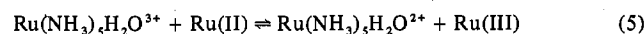
In analogy to other d⁶ hexacoordinate complexes,^{18,20,21} the only primary photosubstitution reaction of Ru(NH₃)₆²⁺ expected is the simple displacement of NH₃ (eq 3). In chloride



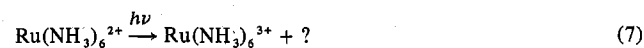
solution the labile equilibrium involving the sixth coordination site is established (eq 4);⁹ however, the equilibrium constant



is sufficiently small that Ru(NH₃)₅H₂O²⁺ is the predominant pentaammineruthenium(II) species in solution.²² Photooxidation may give Ru(NH₃)₆³⁺ or conceivably may be simultaneous with aquation to give Ru(NH₃)₅H₂O³⁺. However, it has been established that, under the experimental concentrations of chloride and catalytic concentrations of Ru(II), any Ru(NH₃)₅H₂O³⁺ formed will be converted to Ru(NH₃)₅Cl²⁺ (λ_{max} 328 nm)^{6,9} according to the equilibria described in eq 5, 4, and 6. At $\lambda_{\text{irr}} \leq 280$ nm very little



Ru(NH₃)₅Cl²⁺ was produced by the photolysis. Thus, the primary photoreaction pathways must be eq 3 and eq 7, and



ruthenium(III) pentaammine complexes, Ru(NH₃)₅Cl²⁺ or Ru(NH₃)₅H₂O³⁺, must result from primary photoaquation (eq 3) followed by rapid secondary oxidation by the Ru(NH₃)₆³⁺ formed independently. A similar conclusion was reached in considering the UV photochemistry of Ru(NH₃)₅CH₃CN²⁺; however, in that case no photoaquation at all was noted with λ_{irr} 214 or 229 nm.⁶

The above analysis leads to the following conclusions regarding the composition of the reaction mixture. When photooxidation (eq 7) is the dominant reaction, the ruthenium species in the reaction mixture are Ru(NH₃)₆²⁺ (starting material), Ru(NH₃)₆³⁺, and Ru(NH₃)₅Cl²⁺. The photoaquation quantum yield is evaluated from the amount of Ru(NH₃)₅Cl²⁺ formed while the photooxidation quantum yield is derived from the total ruthenium(III) formed: Ru(NH₃)₆³⁺ plus Ru(NH₃)₅Cl²⁺. In contrast, when photoaquation is the dominant pathway ($\lambda_{\text{irr}} \geq 313$ nm) the ruthenium species in the photolysis solution are Ru(NH₃)₆²⁺, Ru(NH₃)₅H₂O²⁺, and Ru(NH₃)₅Cl²⁺. Therefore Φ_{ox} is calculated from the concentration of Ru(NH₃)₅Cl²⁺ while Φ_{aq} is derived from the total concentration of pentaammine complexes: Ru(NH₃)₅H₂O²⁺ plus Ru(NH₃)₅Cl²⁺. Spectral analysis at several wavelengths

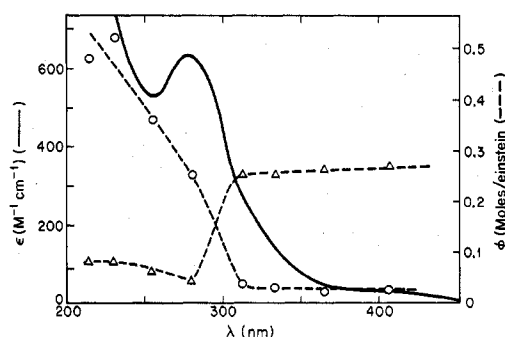


Figure 1. Electronic spectrum of Ru(NH₃)₆²⁺ in 25 °C aqueous solution (0.001 M HCl/0.199 M NaCl). Quantum yields for ammonia aquation Φ_{aq} (triangles) and for photooxidation Φ_{ox} (circles) are plotted as a function of irradiation wavelength.

Table III. Quantum Yields^a Measured for the Photolysis of Aqueous Ru(NH₃)₅H₂O²⁺

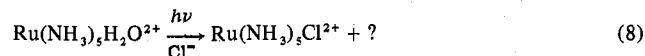
λ_{irr} , nm	Φ_{ox} , mol/einstein	λ_{irr} , nm	Φ_{ox} , mol/einstein
405	0.05 ± 0.01	254	0.22 ± 0.03
366	0.05 ± 0.01	229	0.69 ± 0.05
334	0.03 ± 0.01	214	1.1 ± 0.1
313	0.06 ± 0.01		

^a Measured in 0.001 M HCl/0.199 M NaCl; at 25.0 °C; mean value and average deviation for five or more runs reported.

using the carefully determined molar extinction coefficients of the noted products allows the solution of simultaneous equations¹ to calculate the concentrations of the relevant species as a function of photolysis time in each of the experiments.

Quantum yields Φ_{aq} and Φ_{ox} calculated in this manner for aqueous Ru(NH₃)₆²⁺ are listed in Table II. The most notable feature of these data is the sharp drop in Φ_{aq} and corresponding jump in Φ_{ox} in going from λ_{irr} 313 nm to λ_{irr} 280 nm (Figure 1). In addition, small decreases in both Φ_{ox} and Φ_{aq} are seen when the temperature is lowered from 25 to 6 °C; however, the differences lie within the stated experimental uncertainties. Also, for 366-nm irradiation Φ_{ox} but not Φ_{aq} increases significantly when [H⁺] is raised tenfold. Lastly, addition of 2-propanol (2 M) to the reaction solution appears to decrease both Φ_{ox} and Φ_{aq} for 254-nm photolysis. The effect on Φ_{ox} is somewhat greater.

B. Photolysis of Ru(NH₃)₅H₂O²⁺. Irradiation of Ru(NH₃)₅H₂O²⁺ in deaerated pH 3/0.2 M Cl⁻ solution leads cleanly to the formation of Ru(NH₃)₅Cl²⁺ as the only detectable ruthenium product. The product solution spectrum shows an isosbestic point at 292 nm as expected for eq 8 and



careful analysis of the spectrum at other wavelengths gave no indication of the formation of the Ru(NH₃)₄(H₂O)₂²⁺ or Ru(NH₃)₄Cl₂²⁺ species expected from ammonia photoaquation. On this basis the quantum yield for ammonia photoaquation is estimated to have an upper limit of 0.003 mol/einstein at all λ_{irr} . The quantum yields for Ru(NH₃)₅Cl²⁺ formation (Φ_{ox}) are reported in Table III. Similar to the behavior of Ru(NH₃)₆²⁺, Φ_{ox} is small but real at the irradiation wavelengths ≥ 313 nm and jumps dramatically at shorter wavelengths.

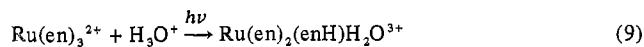
C. Synthesis of Ru(en)₂(enH)Cl³⁺. Photolysis of Ru(en)₃²⁺ in pH 3/0.2 M Cl⁻ solution at 313 or 254 nm gives changes in the electronic spectrum similar to that seen for the analogous irradiation of Ru(NH₃)₆²⁺. Specifically, the photolysis-induced spectral changes involved absorbance decreases for the more intense absorption band of Ru(en)₃²⁺ (302 nm, Table I) and increases at ~345 nm, a wavelength where chloroamine-

Table IV. Quantum Yields^a Measured for the Photolysis of Ru(en)₃²⁺ in Aqueous Solution

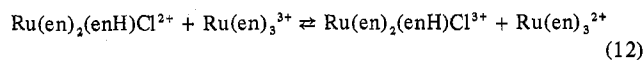
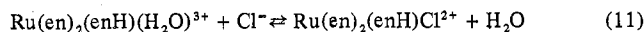
λ_{irr} , nm	Φ_{ox} , mol/einstein	Φ_{aq} , mol/einstein
405	<0.003	0.06 ± 0.01
366	<0.003 (<0.003) ^b	0.06 ± 0.01 (0.031 ± 0.005) ^b
334	0.015 ± 0.002	0.14 ± 0.02
313	0.020 ± 0.002 (0.06 ± 0.01) ^c	0.18 ± 0.01 (0.20 ± 0.02) ^c
280	0.16 ± 0.01	0.03 ± 0.01
254	0.35 ± 0.06	0.04 ± 0.01
229	0.98 ± 0.06	0.07 ± 0.01
214	0.9 ± 0.2	0.06 ± 0.01

^a In 0.001 M HCl/0.199 M NaCl at 25.0 °C unless otherwise stated, mean values and average deviation measured for a minimum of three runs. ^b At 6.0 °C. ^c Measured in 0.010 M HCl/0.190 M NaCl.

ruthenium(III) complexes display strong ligand to metal charge-transfer (LMCT) absorptions.^{3,6} Therefore, in analogy to the reactions described above for Ru(NH₃)₆²⁺ the following primary photoprocesses and secondary reactions may be suggested for Ru(en)₃²⁺:



(where enH⁺ is unidentate ethylenediaminium ion)



The unidentate ethylenediaminium complexes Ru(en)₂(enH)Cl³⁺ and Ru(en)₂(enH)H₂O³⁺ have not previously been reported. Therefore, the photolytic synthesis of [Ru(en)₂(enH)Cl]Cl·ZnCl₄ was undertaken as described in the Experimental Section to demonstrate the viability of the scheme described in eq 9–12 and to obtain spectral information for use in the quantum yield calculations. The material obtained by 254-nm irradiation of [Ru(en)₃]ZnCl₄ in 0.02 M HCl at 5 °C followed by isolation and recrystallization gave a satisfactory elemental analysis for [Ru(en)₂(enH)Cl]Cl·ZnCl₄. The electronic spectrum (Table I) is consistent with that expected for a chloropentaamineruthenium(III) complex (strong LMCT band at 343 nm). Furthermore, reduction of this ion over Zn(Hg) in pH 3 solution followed by neutralization of the acid led to the re-formation of Ru(en)₃²⁺ as observed spectrally. (In acidic solution, the Ru(en)₂(enH)H₂O³⁺ ion is formed.) Since ruthenium(II) amine thermal substitutions generally occur by stereoretentive pathways,⁹ the formation of Ru(en)₃²⁺ implies that the photolysis-formed enH⁺ species have a cis configuration. Formal reduction potentials for the Ru(III)/Ru(II) couples in acidic solution (0.1 M *p*-toluenesulfonic acid/0.1 M potassium *p*-toluenesulfonate) were measured by cyclic voltammetry¹ and found to be 0.15, 0.21, and 0.07 V for Ru(en)₃^{3+/2+}, Ru(en)₂(enH)H₂O^{3+/2+}, and Ru(en)₂(enH)Cl^{3+/2+}, respectively.

D. Quantitative Photolysis of Ru(en)₃²⁺. The scheme described by eq 9–12 predicts that if photooxidation is predominant, the solution resulting from irradiation of Ru(en)₃²⁺ would contain the following species: Ru(en)₃³⁺, Ru(en)₃²⁺, and Ru(en)₂(enH)Cl³⁺. If photoaquation is predominant, the expected solution components are Ru(en)₃²⁺, Ru(en)₂(enH)H₂O³⁺, and Ru(en)₂(enH)Cl³⁺. The dichloro species Ru(en)₂Cl₂⁺ might be expected if the aquation of enH⁺ was rapid; however, under the reaction conditions, Ru(en)₃³⁺, Ru(en)₂(enH)H₂O³⁺, and Ru(en)₂(enH)Cl³⁺ are thermally stable. Therefore analysis of the photolysis solution spectra using several wavelengths and the extinction coefficients

Table V. Product Studies for Hydrogen Gas Formation at 254-nm Irradiation^a

Complex	$n(\text{Ru(III)})^b$	$n(\text{H}_2)^c$	$n(\text{Ru(III)})/n(\text{H}_2)$
Ru(NH ₃) ₆ ²⁺	2.23 × 10 ⁻⁵ 1.75 × 10 ⁻⁵	1.28 × 10 ⁻⁵ 0.71 × 10 ⁻⁵	1.74 2.46
Ru(en) ₃ ²⁺	4.00 × 10 ⁻⁵ 3.88 × 10 ⁻⁵	1.96 × 10 ⁻⁵ 1.73 × 10 ⁻⁵	2.04 2.24
Ru(NH ₃) ₅ H ₂ O ²⁺	1.83 × 10 ⁻⁵ 1.83 × 10 ⁻⁵	1.07 × 10 ⁻⁵ 0.76 × 10 ⁻⁵	1.71 2.41
Ru(NH ₃) ₆ ²⁺ ^d	5.00 × 10 ⁻⁶ 4.74 × 10 ⁻⁶	2.05 × 10 ⁻⁵ 2.33 × 10 ⁻⁵	0.24 0.20

^a Photolysis with UV Products Model PCQ X1 low-pressure mercury lamps at 25 °C. Concentrations were [Ru(II)]₀ ≈ 4 × 10⁻³ M, 0.01 M HCl/0.19 M NaCl in aqueous solution. ^b Number of moles of Ru(III) species formed as determined spectrophotometrically. ^c Number of moles of H₂ produced as measured volumetrically, ideal gas law assumed. ^d In 2 M 2-propanol.

accurately determined for each of the solution components (Ru(en)₂(enH)H₂O³⁺ can be generated in situ from Ru(en)₂(enH)Cl³⁺, see Experimental Section) and solution of the resulting simultaneous equations allow calculations of the relevant quantum yields (Table IV).

The data in Table IV for the photolysis of Ru(en)₃²⁺, although qualitatively similar to those for Ru(NH₃)₆²⁺ (Table II), display several interesting differences. For example, photooxidation is undetectable for λ_{irr} 405 or 366 nm, and the reported value of 0.003 mol/einstein is only an upper limit. Oxidation is notable for 334-nm irradiation and is dominant for $\lambda_{\text{irr}} \leq 280$ nm as was also seen for Ru(NH₃)₆²⁺ and Ru(NH₃)₅H₂O²⁺. The photoaquation yields are larger than Φ_{ox} for $\lambda_{\text{irr}} \geq 313$ nm but show an unusual behavior, starting out at the relatively low value (0.06 mol/einstein) for longer wavelength photolysis (365 and 405 nm), rising to a much higher value (0.18) at λ_{irr} 313, and then dropping again to a lower value (0.03–0.07) at wavelengths where oxidation is the predominant pathway.

The effect of temperature on Φ_{aq} was briefly investigated for 366-nm irradiation. At 6 °C Φ_{aq} is about half the value of 25 °C (Table IV) leading to a calculated apparent activation energy of 5 ± 2 kcal/mol, significantly larger than that seen for the analogous photolysis of Ru(NH₃)₆²⁺. In addition, the effect of [H⁺] was examined for 313-nm irradiation. The value for Φ_{aq} at this wavelength was found the same at pH 2 as at pH 3; however, Φ_{ox} was found to be a factor of 3 larger at the lower pH.

E. Analysis and Quantum Yields of Evolved Gases. Photolysis in the UV region was found to be accompanied by gas evolution for each of the Ru(II) ions studied here. For each case, mass spectral analysis and quantitative volumetric determination of the gas evolved were carried out for photolysis with unfiltered low-pressure mercury lamps. With these lamps >90% of the absorbed radiation is at 253.7 nm. These experiments were conducted in thermostated jacketed cells with deaerated, 0.010 M HCl/0.190 M NaCl, aqueous solution containing the appropriate Ru(II) salt.

Under the above conditions, the mass spectrum of the gas evolving with 253.7-nm irradiation indicated it to have a mass to charge ratio of 2; i.e., the gas is dihydrogen. Results of the volumetric measurements are summarized in Table V for individual experiments where these values can be compared to the spectrally determined quantity of Ru(III) generated in the same photolysis. In each case the Ru(III)/H₂ ratio falls close to 2 although there is significant scatter in the data. The average of these six ratios is 2.1 with a standard deviation of ±0.3. However, when the product studies were carried out for a photolysis solution containing 2 M 2-propanol, it was found that the Ru(III)/H₂ ratios are markedly lower (Table V).

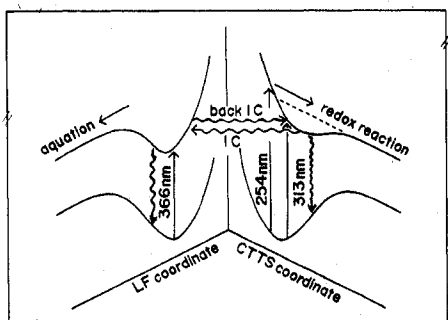


Figure 2. Hypothetical energy surfaces for the excited states of ruthenium(II) amines indicating the view that the aquation and redox pathways derive respectively from ligand field and charge transfer to solvent excited states and that nonradiative deactivation occurs independently from the ligand field and charge-transfer excited-state manifolds.

Discussion

The spectra of $\text{Ru}(\text{NH}_3)_6^{2+}$, $\text{Ru}(\text{NH}_3)_5\text{H}_2\text{O}^{2+}$, and $\text{Ru}(\text{en})_3^{2+}$ in aqueous solution are listed in Table I. Each ion displays a low extinction coefficient shoulder and a much more intense band at higher energy (Figure 1). On the basis of solvent effects on the $\text{Ru}(\text{NH}_3)_6^{2+}$ and $\text{Ru}(\text{en})_3^{2+}$ spectra, we have argued¹¹ that the higher energy bands have substantial charge-transfer character, a point made previously for $\text{Ru}(\text{NH}_3)_6^{2+}$ by Schmidtke.²³ Among the possible charge-transfer transitions, the photochemistry reported here, is consistent with a CTTS assignment (vide infra). The shoulder at ~ 390 nm was assigned^{11,23} to the lower energy, spin-allowed LF band expected for these low-spin d^6 electronic configurations ($^1A_{1g} \rightarrow ^1T_{1g}$ for $\text{Ru}(\text{NH}_3)_6^{2+}$). In addition solvent studies¹¹ did reveal another shoulder in the $\text{Ru}(\text{NH}_3)_6^{2+}$ spectrum at ~ 310 nm which was assigned to the predicted $^1A_{1g} \rightarrow ^1T_{2g}$ transition.

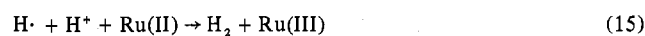
The photoreaction properties of the three ions follow similar patterns although individual differences are in need of discussion. For example, when $\text{Ru}(\text{NH}_3)_6^{2+}$ and $\text{Ru}(\text{NH}_3)_5\text{H}_2\text{O}^{2+}$ are compared, it is seen that the patterns for Φ_{ox} are very similar but that photoaquation is not observable for $\text{Ru}(\text{NH}_3)_5\text{H}_2\text{O}^{2+}$. Two alternative explanations are that $\text{Ru}(\text{NH}_3)_5\text{H}_2\text{O}^{2+}$ does not undergo photolabilization or that the principal photolabilization path involves exchange of coordinated and solvent water. The latter phenomenon is spectrally undetectable and also cannot be studied by isotope labeling studies owing to the thermal lability of the coordinated H_2O .²⁴ Nonetheless, this alternative is the more attractive given studies²⁵ with the isoelectronic rhodium(III) ion $\text{Rh}(\text{NH}_3)_5\text{H}_2\text{O}^{3+}$ which displays considerable photolability of coordinated H_2O but not of NH_3 when irradiated into LF absorption bands.

The quantum yield pattern for $\text{Ru}(\text{NH}_3)_6^{2+}$ shows a marked discontinuity between 313- and 280-nm irradiation. For $\lambda_{\text{irr}} \geq 313$ nm, both Φ_{ox} ($\sim 0.03 \pm 0.01$) and Φ_{aq} ($\sim 0.26 \pm 0.01$) are essentially independent of λ_{irr} . Independence of λ_{irr} suggests population of a common state and that the two reactions represent competitive, first-order deactivation pathways from this state. Since this spectral range corresponds to the LF absorptions, a possible common state would be the lowest energy LF singlet $^1T_{1g}$. A reasonable scenario would be the following: (1) direct excitation into the LF singlet states; (2) relaxation to a common state, e.g., $^1T_{1g}$; (3) aquation via intersystem crossing into the LF triplet states competitive with oxidation via internal conversion from $^1T_{1g}$ into the CTTS state(s). This scenario is illustrated in Figure 2. Ligand photoaquation is consistent with the expected deactivation pathways of d^6 LF states and similar photoaquation is seen^{6,18} for the LF excitation of the isoelectronic $\text{Rh}(\text{NH}_3)_6^{3+}$ and the analogous $\text{Ru}(\text{II})$ species $\text{Ru}(\text{NH}_3)_5\text{CH}_3\text{CN}^{2+}$. In the latter case, irradiation of the lower energy LF band gave no ob-

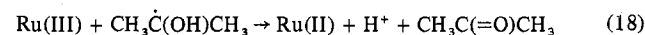
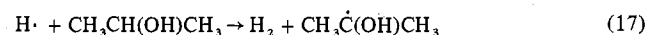
servable photooxidation ($\Phi_{\text{ox}} < 10^{-3}$). However, the $\text{Ru}(\text{III})/\text{Ru}(\text{II})$ reduction potential is considerably larger for $\text{Ru}(\text{NH}_3)_5\text{CH}_3\text{CN}^{3+/2+}$ (0.43 V)²⁶ than for $\text{Ru}(\text{NH}_3)_6^{3+/2+}$ (0.05 V),²⁶ thus making $\text{Ru}(\text{NH}_3)_5\text{CH}_3\text{CN}^{2+}$ the more difficult to oxidize.

The sharp increase in Φ_{ox} and decrease in Φ_{aq} for $\text{Ru}(\text{NH}_3)_6^{2+}$ at 280 nm corresponds to the onset of the CT band in the absorption spectrum (Figure 1). However, while Φ_{ox} has increasing importance at shorter wavelengths, residual photoaquation is also seen. Interestingly, the ratio $\Phi_{\text{aq}}/\Phi_{\text{ox}}$ is approximately constant (~ 0.16) over this wavelength range although the experimental uncertainty in calculating the smaller number is considerable under these conditions. Possible alternative explanations for the observed photoaquation in this region are (1) internal conversion of initially populated CT states into substitution reactive LF states, (2) direct excitation of LF transitions observed by the CT band(s) but still comprising a significant fraction of absorption in that region, or (3) direct reaction from the CT state. Although the last alternative might be suggested by the constant $\Phi_{\text{aq}}/\Phi_{\text{ox}}$ ratio, it is notable that the photooxidation of $\text{Ru}(\text{NH}_3)_5\text{CH}_3\text{CN}^{2+}$ in the same wavelength region is accompanied by little or no photoaquation. Regardless of which of the three alternatives prevail, the Φ_{aq} yields do reveal one important property of the state formed by CT excitation: Since Φ_{aq} is decreased at least threefold from the values seen for direct LF excitation yet oxidation to $\text{Ru}(\text{III})$ represents at most $\sim 50\%$ of the deactivation from the CT state(s) (actually half that value is a more appropriate comparison, vide infra), it is clear that considerable nonradiative deactivation to the ground state is occurring directly from the CT states.

Observation of H_2 as a reaction product with the observed $\Phi_{\text{ox}}/\Phi_{\text{H}_2}$ ratio of 2 is consistent with a reaction scheme such as:



This scheme predicts an upper limit for the quantum yield of $\text{Ru}(\text{III})$ formation (Φ_{ox}) to be 2.0, a prediction consistent with the indication that Φ_{ox} may exceed 1.0 for 214-nm photolysis of $\text{Ru}(\text{NH}_3)_5\text{H}_2\text{O}^{2+}$. Notably in acidic aqueous solution, $\text{H}\cdot$ can oxidize Fe^{2+} to Fe^{3+} ²⁷ and thus is sufficiently powerful to oxidize $\text{Ru}(\text{NH}_3)_6^{2+}$. (In the aqueous chloride media it is conceivable that $\text{Cl}\cdot$ or Cl_2^- will be formed by reaction of $\text{H}\cdot$ with HCl and that these species may serve as the oxidant of $\text{Ru}(\text{II})$.²⁸) The formation of $\text{H}\cdot$ in a reaction such as eq 14 is supported by two observations. First, Φ_{ox} is sensitive to acid concentrations, increasing substantially as $[\text{H}^+]$ is raised, and indicating competition between the trapping of CTTS* by H^+ and relaxation back to starting material. Second, carrying out the reaction in 2 M 2-propanol solution leads to major decreases in the $\Phi_{\text{ox}}/\Phi_{\text{H}_2}$ ratios (Table V) as well as a corresponding decrease in Φ_{ox} (Table II).^{27a} The data indicate trapping of $\text{H}\cdot$ by the alcohol to form a reducing $\text{CH}_3\dot{\text{C}}(\text{OH})\text{CH}_3$ radical which would be expected to react with the $\text{Ru}(\text{III})$ present in solution (eq 17 and 18).²⁹



The excited-state diagram shown in Figure 2, represents the CTTS state as having a discrete energy; however, it must be rather diffuse given the uncertainty and variety of the many solvent/complex configurations in the excited state. The very nature of CTTS states, especially for cationic complexes,

remains a controversial topic. Solvated electrons generally have not been observed in the flash photolysis of cations³⁰ and attempts in our laboratory using a conventional xenon flash apparatus to study aqueous $\text{Ru}(\text{NH}_3)_6^{2+}$ in acidic aqueous solution indicated no transients with lifetimes exceeding 40 μs , especially absorptions attributable to e_{aq}^- . The failure to see e_{aq}^- was certainly no surprise given the rate constants reported for trapping of this species by $\text{Ru}(\text{NH}_3)_6^{3+}$ ($7 \times 10^{10} \text{ M}^{-1} \text{ s}^{-1}$) and by H_{aq}^+ ($2.2 \times 10^{10} \text{ M}^{-1} \text{ s}^{-1}$).³¹ The question remains whether the CTTS state represented in eq 13 and 14 actually involves the formation of a solvated electron or one more tightly bound to the Ru(III) center. However, our view is that the behavior of the system (e.g., the observation of a definite absorption band and the trapability of the CTTS state) suggests the existence of a CTTS state with an energy and configuration loosely defined by a minimum on a potential energy surface as illustrated in Figure 2. Such bound states in which the excited electron is promoted to a spherical potential surface around the central atom are the bases for various theoretical treatments of the CTTS absorptions of halide ions.^{11,30,32,33} The rapidly increasing Φ_{ox} values seen at the shorter irradiation wavelengths are consistent with the higher energy excitation leading to dissociative states with the quantum yields being a function of the excess energy imparted to the reaction fragments.

The photochemistry of $\text{Ru}(\text{en})_3^{2+}$ differs from that of $\text{Ru}(\text{NH}_3)_6^{2+}$ in several important regards, particularly at the longer irradiation wavelengths. First, unlike $\text{Ru}(\text{NH}_3)_6^{2+}$ which shows a wavelength-independent Φ_{ox} at $\lambda_{\text{irr}} > 313 \text{ nm}$, $\text{Ru}(\text{en})_3^{2+}$ shows Φ_{ox} to drop to immeasurable values (< 0.003) at these wavelengths. Similar patterns for Φ_{ox} were seen for the $\text{Ru}(\text{NH}_3)_5(\text{CH}_3\text{CN})^{2+}$ and $\text{Ru}(\text{NH}_3)_5\text{py}^{2+}$ complexes^{5,6} where the failure to see photooxidation for the longer wavelength irradiation (366 and 405 nm) was attributed to the greater difficulty in oxidizing these species as indicated by electrochemical data.²⁶ The tris(ethylenediamine) complex with a $\text{Ru}^{3+/2+}$ reduction potential of +0.15 V is somewhat more difficult to oxidize than $\text{Ru}(\text{NH}_3)_6^{2+}$. However, if an excited-state scheme such as that shown in Figure 2 is indeed applicable, then the differences must lie in the relative rates of reaction or deactivation from the lower energy ligand field and charge-transfer states since absorption spectra (Table I) indicate that the CTTS and lowest LF singlet states may be closer in energy for $\text{Ru}(\text{en})_3^{2+}$ than for $\text{Ru}(\text{NH}_3)_6^{2+}$.

Another difference for $\text{Ru}(\text{en})_3^{2+}$ is the wavelength sensitivity of Φ_{aq} when the complex is irradiated in the λ_{irr} region 405–313 nm. Excitation of the ligand field band at λ_{max} 370 nm with either 366- or 405-nm light gives $\Phi_{\text{aq}} = 0.06$, much smaller than when λ_{irr} is 334 or 313 nm on the lower energy side of the charge-transfer band. We have no ready explanation for this observation other than to suggest that higher energy LF states may be more reactive toward dissociating the nitrogen of the chelating ethylenediamine.

In summary, the photochemical properties of the saturated ammineruthenium(II) complexes can be attributed to two types of excited states, ligand field states from which ligand aquation is one deactivation mode and higher energy charge transfer to solvent states from which oxidation of Ru(II) to Ru(III) with concomitant H_2 formation is a principal deactivation mode. The quantum yield patterns when the charge-transfer absorptions of aqueous $\text{Ru}(\text{NH}_3)_6^{2+}$ are irradiated indicate that the oxidation occurs with the formation of hydrogen atoms, apparently by the reaction of H^+ with the CTTS excited state. We believe that this CTTS state is a bound state with a shallow minimum in its potential energy surface which may be populated by internal conversion from lower energy LF states and may deactivate directly to the ground state. However, the rapidly increasing Φ_{ox} as the irradiation energy is increased through the CT region suggests

that, at the higher energy regions, the CTTS states formed are dissociative in nature and quantum yields for product formation are partly a function of the excess energy imparted to the reaction fragments. Some photooxidation is evident when the lowest energy LF absorptions of $\text{Ru}(\text{NH}_3)_6^{2+}$ and $\text{Ru}(\text{NH}_3)_5\text{H}_2\text{O}^{2+}$ are irradiated and this is interpreted as resulting from back-population of CTTS states from LF states initially populated. The fact that $\text{Ru}(\text{en})_3^{2+}$, $\text{Ru}(\text{NH}_3)_5\text{py}^{2+}$, and $\text{Ru}(\text{NH}_3)_5\text{CH}_3\text{CN}^{2+}$ do not show comparable photooxidation at these wavelengths can be correlated with the more positive Ru(III)/Ru(II) reduction potentials of these species.

Acknowledgment. Preliminary photochemical studies of $\text{Ru}(\text{NH}_3)_6^{2+}$ and $\text{Ru}(\text{en})_3^{2+}$ systems were carried out by R. E. Hintze.¹⁷ This work was supported by the National Science Foundation (Grant CHE 76-00601). We thank Matthey Bishop Co. for a loan of the ruthenium used in this study.

Registry No. $\text{Ru}(\text{NH}_3)_6^{2+}$, 19052-44-9; $\text{Ru}(\text{NH}_3)_5\text{H}_2\text{O}^{2+}$, 21393-88-4; $\text{Ru}(\text{en})_3^{2+}$, 21393-86-2; *cis*- $\text{Ru}(\text{NH}_3)_4(\text{H}_2\text{O})_2^{2+}$, 29946-00-7; *trans*- $\text{Ru}(\text{NH}_3)_4(\text{H}_2\text{O})_2^{2+}$, 42230-44-4; $\text{Ru}(\text{enH})(\text{en})_2(\text{H}_2\text{O})^{2+}$, 66324-40-1; $\text{Ru}(\text{enH})(\text{en})_2\text{Cl}^{3+}$, 66324-39-8; $[\text{Ru}(\text{enH})(\text{en})_2\text{Cl}]\text{Cl}\cdot\text{ZnCl}_4$, 66324-38-7; $[\text{Ru}(\text{enH})(\text{en})_2\text{Cl}]\text{Cl}_3$, 66324-35-4; $[\text{Ru}(\text{en})_3]\text{ZnCl}_4$, 23726-39-8.

References and Notes

- (1) Taken from the Ph.D. dissertation of T.M., University of California, Santa Barbara, 1977.
- (2) Camille and Henry Dreyfus Foundation Teacher Scholar, 1971–1976.
- (3) P. C. Ford, J. D. Petersen, and R. E. Hintze, *Coord. Chem. Rev.*, **14**, 67 (1974).
- (4) (a) P. C. Ford, G. Malouf, J. D. Petersen, and V. A. Durante, *Adv. Chem. Ser.*, No. **150**, 187 (1976); (b) V. A. Durante and P. C. Ford, *J. Am. Chem. Soc.*, **98**, 6898 (1976); (c) G. Malouf and P. C. Ford, *ibid.*, **99**, 7213 (1977).
- (5) R. E. Hintze and P. C. Ford, *Inorg. Chem.*, **14**, 1211 (1975).
- (6) R. E. Hintze and P. C. Ford, *J. Am. Chem. Soc.*, **97**, 2664 (1975).
- (7) J. Van Houten and R. J. Watts, *J. Am. Chem. Soc.*, **98**, 4853 (1976).
- (8) (a) C. Creutz and N. Sutin, *J. Am. Chem. Soc.*, **98**, 6385 (1976); (b) C. T. Lin, W. Böttcher, M. Chau, C. Creutz, and N. Sutin, *ibid.*, **98**, 6536 (1976); (c) P. C. Young, T. J. Meyer, and D. G. Whitten, *ibid.*, **98**, 286 (1976).
- (9) P. C. Ford, *Coord. Chem. Rev.*, **5**, 75 (1970).
- (10) D. A. Chaisson, R. E. Hintze, D. H. Stuermer, J. D. Petersen, D. P. McDonald, and P. C. Ford, *J. Am. Chem. Soc.*, **94**, 6665 (1972).
- (11) T. Matsubara, S. Efrima, H. Metiu, and P. C. Ford, submitted for publication.
- (12) F. M. Lever and A. R. Powell, *J. Chem. Soc. A*, 1477 (1969).
- (13) T. J. Meyer and H. Taube, *Inorg. Chem.*, **7**, 2369 (1968).
- (14) A. D. Allen and C. V. Senoff, *Can. J. Chem.*, **45**, 1337 (1967).
- (15) R. W. Callahan, G. M. Brown, and T. J. Meyer, *Inorg. Chem.*, **14**, 1443 (1975).
- (16) R. G. Gaunder, Ph.D. Dissertation, Stanford University, 1969.
- (17) R. E. Hintze, Ph.D. Dissertation, University of California, Santa Barbara, 1974.
- (18) J. D. Petersen, R. W. Watts, and P. C. Ford, *J. Am. Chem. Soc.*, **98**, 3188 (1976).
- (19) D. D. Davis and K. L. Stevenson, *J. Chem. Educ.*, **54**, 394 (1977). We thank K. L. Stevenson for a copy of the manuscript prior to publication.
- (20) A. W. Adamson and P. D. Fleischauer, Eds., "Concepts of Inorganic Photochemistry", Wiley-Interscience, New York, N.Y., 1975.
- (21) V. Balzani and V. Carassiti, "Photochemistry of Coordination Compounds", Academic Press, New York, N.Y., 1970.
- (22) G. N. Coleman, J. W. Gesler, F. A. Shirley, and J. R. Kuempel, *Inorg. Chem.*, **12**, 1036 (1973).
- (23) H. H. Schmidtke and D. Garthoff, *Helv. Chim. Acta*, **49**, 2039 (1966).
- (24) R. J. Allen and P. C. Ford, *Inorg. Chem.*, **11**, 679 (1972).
- (25) P. C. Ford and J. D. Petersen, *Inorg. Chem.*, **14**, 1404 (1975).
- (26) T. Matsubara and P. C. Ford, *Inorg. Chem.*, **15**, 1107 (1976).
- (27) (a) A. J. Swallow, "Radiation Chemistry", Halsted Press, London, 1973, p 159; (b) G. Czapski, J. Jortner, and G. Stein, *J. Phys. Chem.*, **65**, 960 (1961).
- (28) D. Meyerstein, private communication.
- (29) D. H. Baxendale, M. A. J. Rodgers, and M. D. Ward, *J. Chem. Soc. A*, 1246 (1970).
- (30) M. Fox, ref 20, Chapter 8.
- (31) E. J. Hart and M. Anbar, "The Hydrated Electron", Wiley-Interscience, New York, N.Y., 1970.
- (32) (a) J. Jortner and A. Treinen, *Trans. Faraday Soc.*, **58**, 1503 (1962); (b) A. G. El-Kourasky and R. Grinter, *J. Chem. Soc., Faraday Trans. 2*, **73**, 1050 (1977).
- (33) C. K. Jorgensen in "Halogen Chemistry", Vol. 1, V. Gutmann, Ed., Academic Press, London, 1967, Chapter 5.